Chin. J. Mech. Eng. (2017) 30:1426–1437
https://doi.org/10.1007/s10033-017-0195-0

ORIGINAL ARTICLE

Phase-Division-Based Dynamic Optimization of Linkages for Drawing Servo Presses

Zhi-Gang Zhang[1,2] · Li-Ping Wang[2] · Yan-Ke Cao[1]

Received: 30 September 2016 / Revised: 22 June 2017 / Accepted: 11 October 2017 / Published online: 10 November 2017

Abstract Existing linkage-optimization methods are designed for mechanical presses; few can be directly used for servo presses, so development of the servo press is limited. Based on the complementarity of linkage optimization and motion planning, a phase-division-based linkage-optimization model for a drawing servo press is established. Considering the motion-planning principles of a drawing servo press, and taking account of work rating and efficiency, the constraints of the optimization model are constructed. Linkage is optimized in two modes: use of either constant eccentric speed or constant slide speed in the work segments. The performances of optimized linkages are compared with those of a mature linkage SL4-2000A, which is optimized by a traditional method. The results show that the work rating of a drawing servo press equipped with linkages optimized by this new method improved and the root-mean-square torque of the servo motors is reduced by more than 10%. This research provides a promising method for designing energy-saving drawing servo presses with high work ratings.

Keywords Drawing servo press · Linkage optimization · Phase-division · Motion planning

Supported by National Science and Technology Major Project of the Ministry of Science and Technology of China (Grant No. 2015ZX04003004).

✉ Zhi-Gang Zhang
zhang_zhigang@jiermt.com

[1] JIER Machine-Tool Group Co., Ltd, Jinan 250022, China

[2] Department of Mechanical Engineering, Tsinghua University, Beijing 100084, China

1 Introduction

Mechanical drawing presses are highly efficient and widely used for sheet metal drawing. With the development of automated technology, drawing and other presses with various functions have been integrated into stamping lines. The slide speed of a drawing press needs to meet the limitations of drawing speed and accommodate the high productivity of the stamping line, so the idle slide stroke time needs to be as short as possible. To fulfill this purpose, a multi-bar linkage is generally used for the drive system [1–3]. At present, most large drawing presses for sheet metal, both in China and abroad, adopt six- or eight-bar linkages; however, because of inherent geometric and structural limitations of the linkage mechanism, the work rating and efficiency of mechanical presses have been limited [4–6].

Use of a servo press can overcome the above shortcomings [7]. Along with servo-drive control, a wide range of movements can be executed with improved accuracy and the slide speed can be freely controlled, endowing the slide with variable motion features that can overcome the intrinsic limitations of the linkage mechanism in motion curves and enable the servo press to better match high-speed feeding systems [8–11]. In addition, good coordination between the servo-drive system and its linkages can decrease motor power and energy consumption of the drive system [12–14]. Based on these features, stamping lines equipped with drawing servo presses routinely break productivity records in various industries.

At present, the Stephenson six-bar linkage is commonly used on large drawing servo presses. Its structure is same as that of a traditional six-bar linkage mechanical press. To obtain optimum matching between the servo-drive system and linkages, linkage optimization is necessary for the drawing servo press. Zhou proposed an objective function

method and used it to optimize the mechanism of a servo punch press [15, 16]. Mundo proposed a method for the synthesis of planar mechanisms: the optimized mechanism was able to move a press ram according to an optimal law of motion [17]. Du used an inheritance calculation method to optimize linkage of a press [18]. Although optimization of linkage has been studied and discussed worldwide, few results have been practically applied [19–22]. Further research on linkage optimization of drawing servo presses is still needed.

This paper aims to provide a new method for linkage optimization of a drawing servo press. The objective function and constraints were established based on a motion phase-division model of a servo press. Original data and a research methodology for the design and application of a drawing servo press are provided.

2 Methods

2.1 Phase-Division of Slide Motion

Basing on the drawing process, the slide motion of a drawing servo press was phase-divided into four segments: the work segment (*SegWork*), feeding segment (*SegFeed*), deceleration segment (*SegDec*), and back-acceleration segment (*SegBkAcc*), as shown in Figure 1. The principles corresponding to each segment were considered in the process of motion planning, as listed in Table 1.

Motion planning for the drawing servo press aimed to obtain the curves of eccentric motion, which can coordinate with other servo presses in the stamping line to achieve the set work rating. Optimization of linkage, such as implementing good technological properties, high work rating, and low vibration and noise, can enable the motion planning to more easily obtain high-quality motion curves. The linkage-optimization principles should therefore be established based on the principles of motion planning.

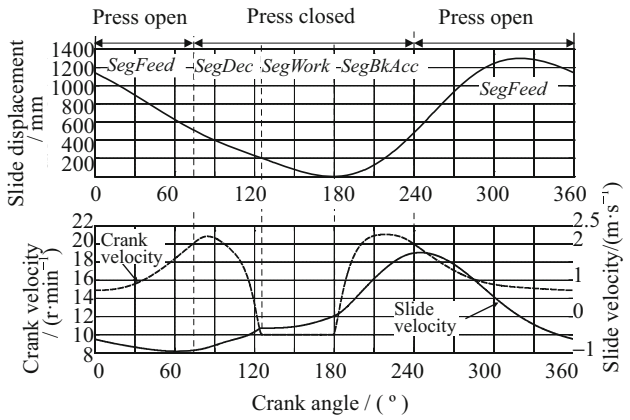

Figure 1 Phase-division of drawing servo press slide motion

2.2 Constraints of Linkage Optimization

Using the principles of motion planning, linkage-optimization principles for a drawing servo press are proposed, as listed in Table 2.

Based on these principles, the objective functions and constraints were defined as follows.

2.2.1 Constraints of Slide Displacement

The relationship between slide displacement and velocity was defined as follows:

$$f_1(X) = \int_{\varphi_{S_c}}^{\varphi_{S_p}} [Vs(\varphi) - Vs_{\mathrm{WkC}}]^2 \mathrm{d}\varphi, \tag{1}$$

where φ_{S_c} is the angle corresponding to the maximum work stroke, φ_{S_p} is the angle corresponding to the nominal stroke. $Vs(\varphi)$ is the slide velocity function, and X is an optimized parameter vector.

S_c and S_p meet the following constraints respectively:

$$h_1(X) = s(\varphi_{S_c}) - S_c = 0, \tag{2}$$

$$h_2(X) = s(\varphi_{S_p}) - S_p = 0, \tag{3}$$

where S_p is the nominal stroke, S_c is the maximum work stroke, and $s(\varphi)$ is the slide displacement function.

2.2.2 Constraints of Slide Velocity

The friction loss of the linkage joint in *SegWork* can be expressed using the following function:

$$f_2(X) = \sum_{j=1}^{N_j} \int_{\varphi_{Sc}}^{\varphi_{\mathrm{BDC}}} \frac{\mu_j D_j}{2} F_{R,j}(\varphi)\Omega_j(\varphi)\mathrm{d}\varphi, \tag{4}$$

where $F_{R,j}(\varphi)$ is the radial force of joint j, $\Omega_j(\varphi) = \omega_j(t)/\omega_{\mathrm{ECC}}$ is the similar velocity of joint j, φ_{BDC} is the angle at bottom dead center (BDC), μ_j is the friction coefficient of joint j, and D_j is the diameter of joint j.

The constraints at BDC and top dead center (TDC) are defined as:

$$h_3(X) = Vs(\varphi_{\mathrm{BDC}}) = 0, \tag{5}$$

$$h_4(X) = Vs(\varphi_{\mathrm{TDC}}) = 0, \tag{6}$$

where φ_{TDC} is the angle at TDC. The friction between the slide and the gib can be ignored for two-point and four-point presses.

2.2.3 Constraints of Ideal Equivalent Force Arm

The ideal equivalent force arm (m_{IE}) is given by:

$$m_{\mathrm{IE}} = \frac{M_I}{P_n} = Vs(\varphi_{S_p}), \tag{7}$$

Table 1 Motion-planning principles corresponding to four defined phase-divided segments

Phase division	Principles of motion planning
SegWork	Required slide speed being reached as precondition, slide running time in this segment should be as short as possible and the mechanism friction energy loss should be as low as possible
SegFeed	The time and space should be sufficient for the feeding device to move in the die area, and the fluctuation of eccentric speed should be minimized
SegDec and *SegBkAcc*	The time for realizing work rating being met as precondition, the energy consumption should be minimized, emergency stop (E-stop) and braking time requirement should be met

Table 2 Linkage-optimization principles corresponding to motion-planning principles

Phase division	Principles of motion planning	Principles of linkage optimization
SegWork	Slide speed meets technological requirements and slide running time in this segment is as short as possible	The slide velocity Vs_{WkC} in *SegWork* is constant and the corresponding slide displacement should be as long as possible in the work stroke S_c
	Energy loss due to mechanism friction in *SegWork* should be as low as possible	In *SegWork*, friction loss of linkage joints based on set load curve should be kept lowest
		Ideal equivalent arm m_{IE} should be small
SegFeed	Consistent with feeding motion; velocity fluctuation should be minimized	The open height and open angle of die satisfy defined constraints
	Vibration and noise	The max acceleration of slide near the top dead center and linkage pressure angle meet defined constraints
SegDec and *SegBkAcc*	Required work rating is met, energy consumption should be minimized	The equivalent inertia of linkage should be as low as possible; equivalent inertia including slide and upper die weight should be as low as possible
		Eccentric rotary speed should be fast and Vs_{WkC} should be slow in *SegWork*, respectively
	E-stop and braking time being met.	Downward equivalent inertia with slide and upper die weight should be as low as possible

where M_I is the ideal press nominal torque and P_n is the press capacity.

Ideal equivalent force arm can significantly influence the gear inertia and servo motor torque. The constraint is defined as:

$$g_1(X) = m_{\mathrm{IE}} - C_1 \le 0, \tag{8}$$

where C_1 is a constant.

2.2.4 Constraints in SegFeed

The open height (h_A) and closed height (h_p) of the die meet the following constraints:

$$h_5(X) = s(\varphi_p) - h_p = 0, \tag{9}$$

$$h_6(X) = s(\varphi_A) - h_A = 0, \tag{10}$$

where φ_p and φ_A are the eccentric angles corresponding to die closure and opening, respectively.

The constraint of φ_A and φ_p can be defined as follows (C_2 is a constant):

$$g_2(X) = C_2 - (\varphi_A - \varphi_P) \le 0. \tag{11}$$

Maximum acceleration of the slide near TDC meets the following constraint (C_3 is a constant):

$$g_3(X) = C_3 - \inf\{g(\varphi)|\varphi \in [0, 2\pi]\} \le 0. \tag{12}$$

The constraints of the linkage pressure angles are given by:

$$g_4(X) = C_4 - \inf\left\{\theta_{J7}(\varphi)\middle|\varphi \in \left[\varphi_{S_c}, \varphi_{\mathrm{BDC}}\right]\right\} \le 0, \tag{13}$$

$$g_5(X) = \sup\left\{\theta_{J7}(\varphi)\middle|\varphi \in \left[\varphi_{S_c}, \varphi_{\mathrm{BDC}}\right]\right\} - C_5 \le 0, \tag{14}$$

where $\theta_{J7}(\varphi)$ is the inclination between the linkage axis and vertical direction and C_4 and C_5 are constant values.

2.2.5 Constraints of Equivalent Inertia

The linkage inertia equation is given by:

$$f_3(X) = \sup\{Je_{\mathrm{Lk}}(\varphi)|\varphi \in [0, 2\pi]\} - C_{\mathrm{JeL}}, \tag{15}$$

where $Je_{\mathrm{LK}}(\varphi)$ is the equivalent inertial of linkage as a function of eccentric angle C_{JeL} is a constant.

Maximum equivalent downward inertia with slide and die is given by:

$$f_4(X) = \sup\{Je_s(\varphi)|\varphi \in [\varphi_{\mathrm{TDC}} - 2\pi, \varphi_{\mathrm{BDC}}]\} - C_{\mathrm{Jd}}, \quad (16)$$

where $Je_s(\varphi)$ is the equivalent inertial of the linkage, slide, and tool as a function of eccentric angle and C_{Jd} is a constant.

Maximum equivalent inertia in the back stroke with slide and die (C_{Ju} is a constant) is given by:

$$f_5(X) = \sup\{Je_s(\varphi)|\varphi \in [\varphi_{\mathrm{BDC}}, \varphi_{\mathrm{TDC}}]\} - C_{\mathrm{Ju}}. \quad (17)$$

2.2.6 Slide Velocity in SegWork

Slide constant velocity, Vs_{WkC}, in *SegWork* was taken as a design parameter.

2.2.7 Other Constraints

Other constraints included: a size constraint for the linkage component; a space-size constraint for linkage components at limited position; a total stroke constraint for the slide; a constraint for the slide in the linkage group [23].

2.3 Objectives of Linkage Optimization

The unknown variable X included nine size variables of the six-bar linkage (R, X_2, Y_2, L_2, X_3, L_{42}, L_{45}, Ang_4, L_5), where

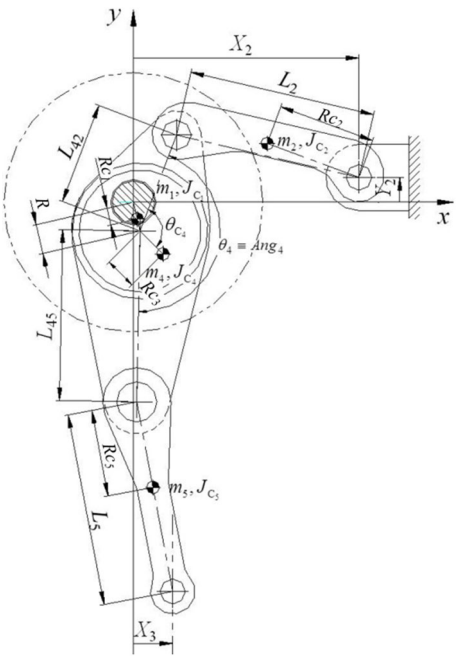

Figure 2 Structure and size parameters of six-bar linkage used for drawing servo press

R is crank length, X_2 is horizontal distance from the pull-bar shaft to the eccentric shaft, Y_2 is vertical distance from pull-bar shaft to eccentric shaft, L_2 is pull-bar length, X_3 is the horizontal deviation of the small-end axis of the link to the eccentric shaft, L_{42} is the upper-arm length of the angle plate, L_{45} is the lower-arm length of the angle plate, Ang_4 is the inclination between the upper and lower arms of the angle plate, and L_5 is the length of connecting rod, as shown in Figure 2. The phase-division angles included φ_{TDC}, φ_P, φ_{S_c}, φ_{S_p}, φ_{BDC}, and φ_A.

The objectives of six-bar linkage optimization were defined as follows:

$$\min_{X \in R^{15}} F(X) = \sum_i w_i f_i(X), \quad (18)$$

$$s.t. g_u(X) \leq 0 (u = 1, 2, \ldots 5, \ldots), \quad (19)$$

$$h_v(X) = 0 (v = 1, 2, \ldots 5, \ldots). \quad (20)$$

Owing to the large number and complexity of the constraints, it is difficult to find suitable results for certain conditions. The interior-point algorithm of the non-linear constraint optimization function, *fmincon*, in *MATLAB*$^{\mathrm{TM}}$ was therefore used to solve the above problems.

2.4 Method for Calculation of Equivalent Inertia

The linkage components used on drawing servo presses are often irregularly shaped, as shown in Figure 2. The mass and inertia of each component needs to be calculated at each iteration in the process of dynamic optimization. It is therefore essential to efficiently and precisely obtain the mass, mass center position, and rotary inertia of each component [24]. In this paper, a convenient method is proposed to obtain these parameters. The components are divided into trapezoid and truncated cones, where the areas of the new parts can be either positive or negative (negative means that material is removed), as shown in Figure 3. It is easier to obtain analytical expressions for the first and second moments to origin of these two shapes.

This division method is suitable for planar linkages and even for eccentric complex shapes. The inertia calculation based on this method achieves a high level of accuracy: it has better accuracy than three-dimensional inertia calculation models. Eqs. (15)–(17), used for calculation of inertia, are based on this method.

2.5 Treatment of Linkage Joint Friction Loss

The force analysis of a six-bar linkage is a nonlinear problem: iteration is required to obtain a solution. Taking friction into account in the process of force analysis will

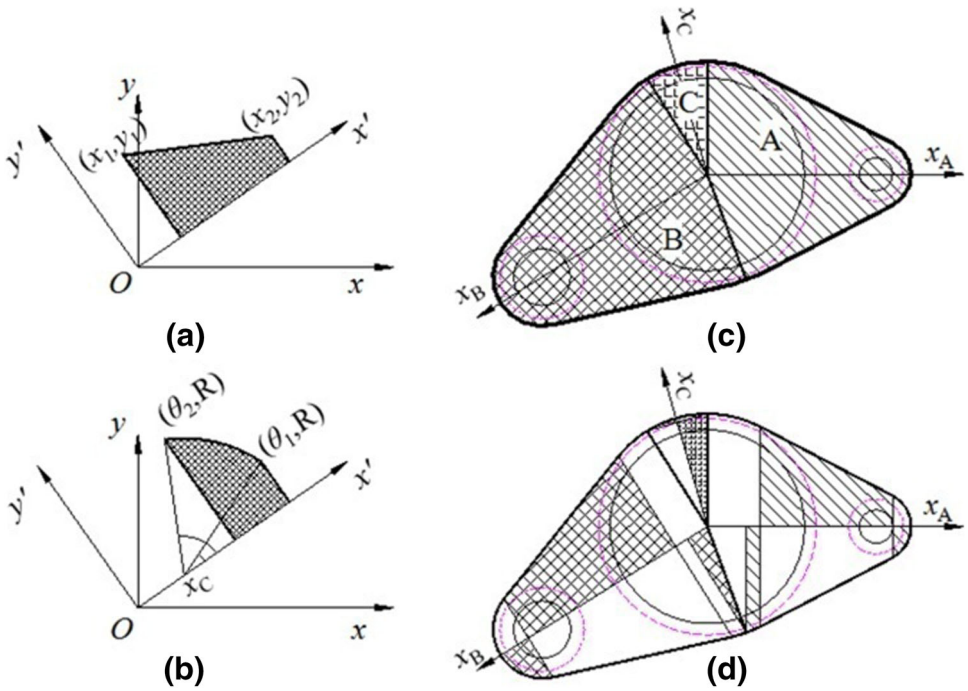

Figure 3 Area moment of trapezoid and truncated cone to origin: (a) origin moment of trapezoid; (b) origin moment of truncated cone; (c) linkage shape division by different axis zone; (d) division of axis zones

decrease the efficiency of solution of linkage optimization. To improve the efficiency of the solution process, a dynamic static force analysis method was employed to calculate the radial forces of joints, ignoring the joint friction. After optimization, dynamic simulation could then be used to verify the reduction of friction loss due to optimization.

2.6 Assignment of Initial Value

To test the stability of this proposed calculation method and evaluate its capability to obtain a solution from any initial value, the size of a similar six-bar linkage obtained by ruler measurement on a technical document was used as the initial value, as shown in Figure 4. Because the initial value was roughly measured by ruler, the data error was large, as listed in Table 3.

3 Case Study

The first 20 MN drawing servo press (SL4-2000A) in China, made by JIER (JIER Machine-Tool Group Co., Ltd), was used to demonstrate this optimization method. The capacity of the press is 20 MN, its nominal working stroke is 8 mm, the slide stroke is 1300 mm, and there are 15 slide strokes per minute. Its transmission system uses a six-bar linkage (Figure 2) that was precisely optimized by traditional methods during the design stage [25, 26]. In this paper, the six-bar linkage was again optimized using the as-proposed method.

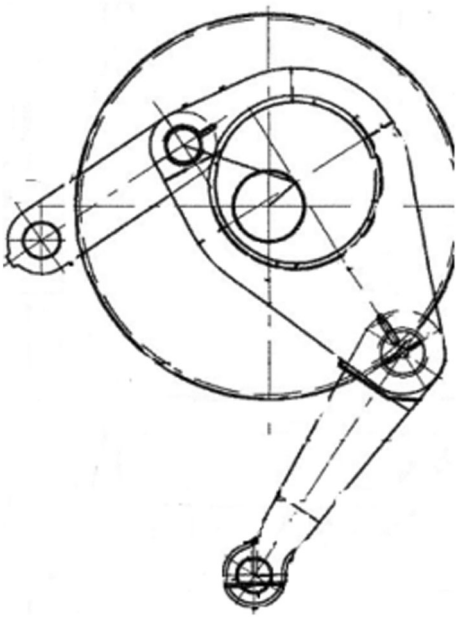

Figure 4 Image of six-bar linkage in technical document

4 Results and Discussion

4.1 Optimization Based on Constant-eccentric-speed Mode

Use of constant eccentric speed at *SegWork* is the basic work mode (constant-eccentric-speed mode) of this drawing servo press, which is beneficial to the full conversion of motor torque to forming force in the drawing process. If a

Table 3 Sizes of optimized linkage based on constant-eccentric-speed mode

Parameter	Initial value X_0	Optimized result $X_{OPTIMAL}$		
		Lk_1	Lk_2	Lk_3
R	260	333.369	328.498	332.853
L_2	1274	871.589	1309.244	1173.824
X_2	1700	1345.486	1800.000	1653.934
Y_2	–260	138.929	–239.767	–175.091
X_3	140	51.280	260.000	258.486
L_{42}	899	998.369	993.498	997.853
L_{45}	1510	1291.617	1527.851	1367.032
Ang_4	–140	–153.794	–138.841	–139.191
L_5	2025	1501.651	1832.239	1682.866

six-bar linkage is designed in constant-eccentric-speed mode, the ideal motion curve is that in which the slide velocity is kept constant in *SegWork*, as shown in Table 2.

The validity of the optimization method in constant-eccentric-speed mode was verified in two ways: by optimizing under the same design parameters as those of the SL4-2000A and by optimizing under different design parameters.

4.1.1 Optimization under Same Design Parameters as SL4-2000A

When the SL4-2000A eccentric rotates at a constant speed of 1 rad/s, the corresponding slide velocity at *SegWork* is about 303 mm/s. Linkage optimization in this section was therefore carried out using S_c = 300 mm (maximum work stroke) and Vs_{WkC}=300 mm/s (slide velocity in *Segwork*). The simulated load in the work strokes used for motion planning is shown in Figure 5.

The sizes of linkage Lk_1 optimized by the above method are shown in Table 3. The actual SL4-2000A linkage size is proprietary knowledge of JIER, so cannot be revealed here; however, the performances of the two linkages were compared as follows.

The slide velocity in *SegWork* and slide displacement of optimized linkage Lk_1 coincided well with those of SL4-2000A, as shown in Figs. 6 and 7, respectively. Basic parameters of linkages Lk_1 and SL4-2000A are listed in Table 4, from which it is easily shown that, even if starting from a rough initial value, the proposed optimization method can still obtain a solution that is extremely close to that of the mature linkage of SL4-2000A.

When the slide work stroke was 300 mm (S_{wk} = 300 mm), the maximum work rating of the drawing servo press equipped with linkage Lk_1 was about 15 s/min, which was

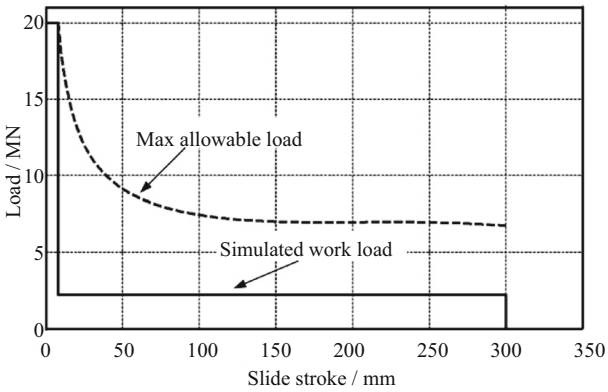

Figure 5 Simulated load for work stroke of 300 mm

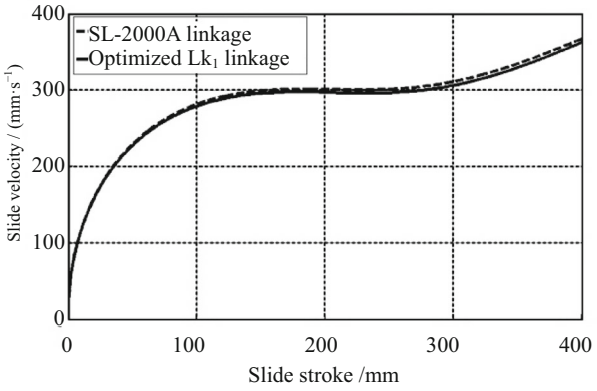

Figure 6 Comparison of slide velocity in *SegWork*

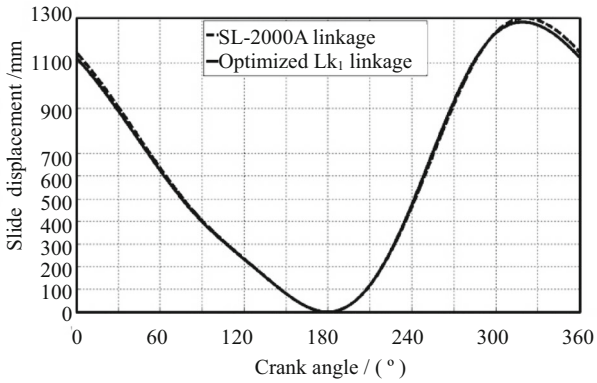

Figure 7 Comparison of slide displacement

equivalent to that of the 20 MN drawing servo press (SL4-2000A); however, the root-mean-square value of torque of linkage Lk_1 was 3.4% lower, as shown in Table 5. Under the conditions of S_{wk} = 300 mm and Nc = 15 s/min, the motion-planning curves of linkage Lk_1 are shown in Figure 8. The above results indicate the validity of the optimization method in constant-eccentric-speed mode.

Table 4 Comparison of basic parameters for optimized linkage Lk_1 and SL4-2000A

Mechanism	*SegWork* constant velocity	System inertia	Mechanism inertia	*SegWork* friction power	Die area open angle	Ideal equivalent force arm	
	Vs_{WkC} / (mm·s^{-1})	Je_{Max}/ (kg·m^2)	Je_{LkMax}/ (kg·m^2)	W_{FrcWk} / kJ	$\Delta\Phi_{feed}$ / (°)	m_{IE13} / mm	m_{IE8} / mm
SL4-2000A	≈303	19900.6	4398.7	6040.3	175.3	130.7	104.5
Lk_1	300	20229.7	4371.2	6037.6	175.0	130.0	104.1

Table 5 Motion-planning results for optimized linkage Lk_1

Linkage	Max work rating planning Nc_{max} / (s·min^{-1}) S_{wk}=300 mm	Optimization of root-mean-square torque T_{drms}/ (N·m) S_{wk}=300 mm, Nc=15 s·min^{-1}
SL4-2000A	15.189	8215.4
Lk_1	15.242	7934.7

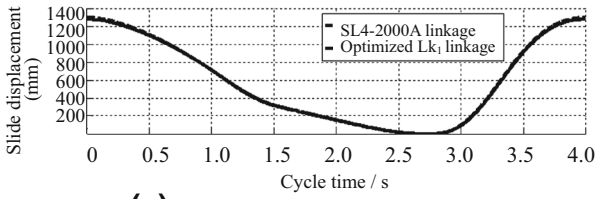

(a) Slide displacement in a single cycle

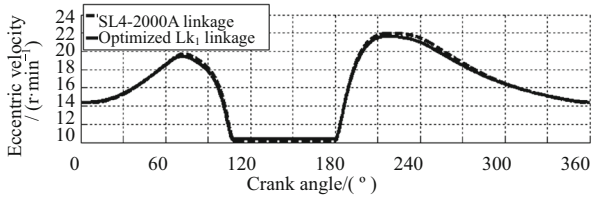

(b) Eccentric velocity as a function of crank angle

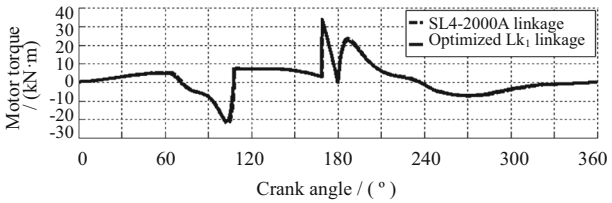

(c) Motor torque as a function of crank angle

Figure 8 Motion-planning curves based on S_{wk} = 300 mm and Nc = 15 r/min

4.1.2 Optimization under Design Parameters Differing from SL4-2000A

In Section 4.1.1, the major difference identified between optimized linkage Lk_1 and that of SL4-2000A was that the former had slightly lower velocity Vs_{WkC} in *SegWork*, which is beneficial to improving stamping quality. This study therefore aimed to lower velocity Vs_{WkC} while maintaining the equivalent inertia as low as possible, thereby decreasing energy consumption during the acceleration and deceleration segments.

Under the conditions of S_c = 300 mm, Vs_{WkC} = 280 mm/s, and a different die open angle, optimized linkages Lk_2 and Lk_3 were obtained, the sizes and basic parameters of which are shown in Tables 3 and 6, respectively. Compared with SL4-2000A, the inertias of linkages Lk_2 and Lk_3 slightly increased due to the decrease of Vs_{WkC} (Table 6); however, the root-mean-square value of torque was significantly decreased, as shown in Table 7. Under the condition of S_{wk}=300 mm and Nc=15 s/min, the root-mean-square torque of linkage Lk_2 was more than 10% smaller than that of SL4-2000A; for linkage Lk_3, the value was 5.2% smaller. Moreover, compared with SL4-2000A, the ideal equivalent force arm of linkages Lk_2 and Lk_3 also decreased, resulting in a decrease of the gear system design load, which is beneficial to lifetime extension and weight reduction of the gear system. Taking linkage Lk_2 as an example, the motion-planning curves are shown in Figure 9.

According to the above results and analyses, the following conclusions can be drawn. If the basic work mode of a drawing servo press employs constant-eccentric- speed in *SegWork*, the slide speed of a drawing servo press equipped with a linkage optimized by the above method can approach ideal during the work phase. This optimization method can precisely control Vs_{WkC}, the ideal force arm, and the friction consumption of the linkage in *SegWork*, without obviously increasing the moments of inertia.

Table 6 Comparison of basic parameters for optimized linkages Lk_2 and Lk_3 and SL4-2000A

Mechanism	Max work stroke	*SegWork* constant velocity	Die area open angle	System inertia	Mechanism inertia	*SegWork* friction power	Ideal equivalent force arm	
	S_c/ mm	Vs_{WkC}/(mm·s^{-1})	$\Delta\Phi_{feed}$/ (°)	Je_{Max}/ (kg·m^2)	Je_{LkMax}/ (kg·m^2)	W_{FrcWk}/kJ	m_{IE13}/ mm	m_{IE8}/ mm
SL4-2000A	300	≈303	175.3	19900.6	4398.7	6040.3	130.7	104.5
Lk2	300	280	170.0	24636.6	4974.4	6037.6	125.6	100.9
Lk3	300	280	167.5	21555.8	4565.5	6037.6	124.8	100.2

Table 7 Motion-planning results for optimized linkages Lk_2 and Lk_3

Linkage	Max work rating planning Nc_{max}/(s·min^{-1}) S_{wk}=300 mm	Optimization of root-mean-square torque T_{drms}/ (N·m) S_{wk}=300 mm, Nc=15 s/min
SL4-2000A	15.189	8215.4
Lk_2	15.317	7383.0
Lk_3	15.229	7787.9

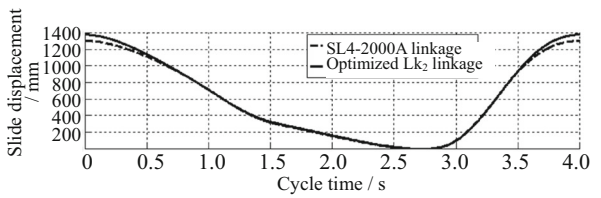

(a) Slide displacement in a single cycle

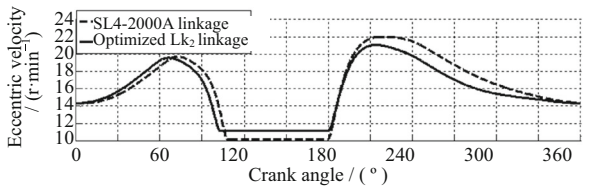

(b) Eccentric velocity as a function of crank angle

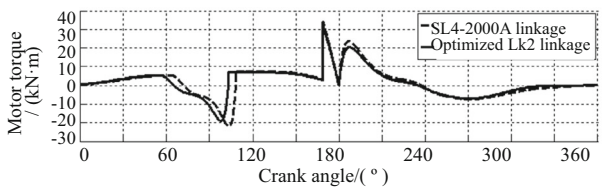

(c) Motor torque as a function of crank angle

Figure 9 Motion-planning curves based on S_{wk} = 300 mm and Nc = 15 s/min

During the process of optimization, the speed and ideal force arm can be selected as needed. This method has advantages over the traditional method in its ability to improve energy saving and running efficiency of a linkage. In addition, servo motion planning techniques can be merged into the linkage-optimization process as a reference for selection of linkage-optimization parameters, thereby comprehensively improving the properties of the different phases.

4.2 Optimization Based on Constant-slide-speed Mode

The typical characteristic of slide velocity in *SegWork* is shown in Figure 6: slide velocity Vs_{WkC} fluctuates in the segment and the slide stroke corresponding to constant velocity Vs_{WkC} is too short (only about half of the maximum work stroke). Owing to the limitations of a six-bar linkage, traditional mechanical presses cannot overcome these two shortcomings; however, the drawing servo press can overcome these by motion planning in constant-slide-speed mode. A schematic diagram of slide speed control is given in Figure 10.

Using a servo-controlled system, the constant-slide-speed region can be extended and speed fluctuations in this region will decrease. Nevertheless, control of slide speed in *SegWork* should not affect the nominal torque output capability of the press: only surplus torque of the motor is allowed to be used for controlling the slide speed in *SegWork*, as shown in Figure 11.

The implication of using constant-slide-speed mode lies in the fact that the work rating can be greatly increased and energy consumption of the motor and drive system decreased, while the load-bearing capability of the servo press and the motor capability remain almost the same. Motion-planning results of optimized linkages Lk_1 to Lk_3 in the different modes are shown in Table 8. Under the same work stroke, slide work velocity, and feeding time, one additional work rating was achieved per minute and energy consumption of the motor and drive decreased by 40% in constant-slide-speed mode.

The above results indicate that motion planning in constant-slide-speed mode can overcome the inherent

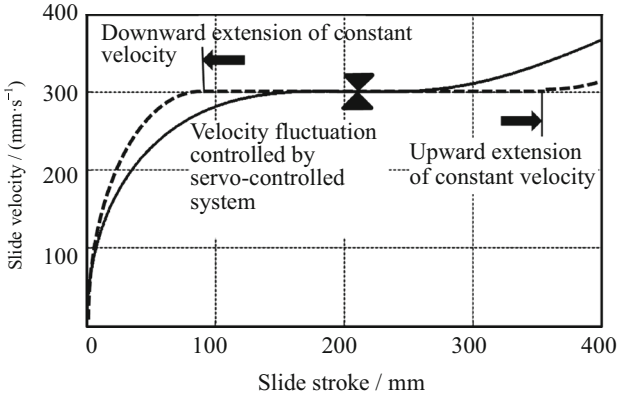

Figure 10 Extension of constant-velocity region by use of servo-control system

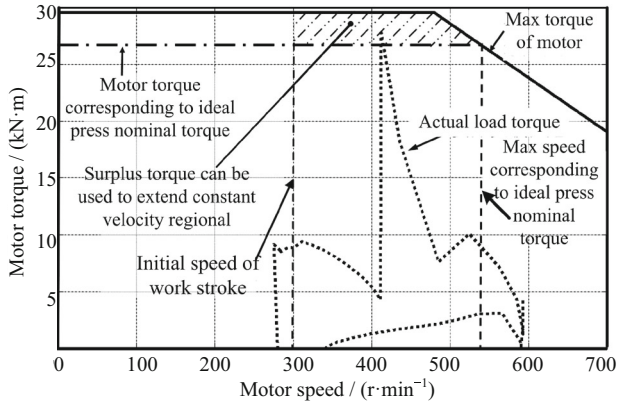

Figure 11 Torque compatibility principle for constant-slide speed control

shortcomings of linkages, offering more choices with respect to increasing the speed and energy saving.

To obtain consistency with the constant-slide-speed mode in *SegWork*, the following constraint can be added to the linkage inertia optimization, improving the acceleration performance of the linkage in *SegWork*:

$$f_{3b}(X) = \frac{1}{\varphi_{\mathrm{BDC}} - \varphi_{\mathrm{WkS}}} \int_{\varphi_{\mathrm{WkS}}}^{\varphi_{\mathrm{BDC}}} Je_{\mathrm{Lk}}(\varphi)\mathrm{d}\varphi. \tag{21}$$

Linkage sizes for Lk_4 and Lk_5, optimized in constant-slide-speed mode, are shown in Table 9 for conditions of different work strokes, slide speeds in *SegWork*, and die open angles.

Features of linkages Lk_4 and Lk_5 are shown in Table 10. Optimization in constant-slide-speed mode can lower the slide velocity in *SegWork* and ideal equivalent force arm of linkage, while keeping the equivalent inertia almost constant.

Motion-planning results for linkages Lk_4 and Lk_5 optimized in constant-slide-speed mode are shown in Table 11, which shows that the work rating of a drawing servo press

Table 8 Motion-planning results of for different modes

Mechanism	Eccentric constant speed mode (S300)		Constant slide speed mode (S300)		
	$Nc_{\max}$/ (s·min^{-1})	Td_r/ (N·m)	$Nc_{\max}$/ (s·min^{-1})	Td_r'/ (N·m)	$\frac{Td_r'}{Td_r} - 1$
SL4-2000A	15.189	9433.8	16.118	6075.4	-36%
Lk_1	15.242	9451.3	16.152	5964.2	-37%
Lk_2	15.317	9224.2	16.119	5786.9	-37%
Lk_3	15.229	9124.2	16.124	5632.1	-38%

Table 9 Sizes of optimized linkages in constant-slide-speed mode

Parameter	Initial value	Optimized result X_{OPTIMAL}	
	X_0	Lk_4	Lk_5
R	260	334.526	295.785
L_2	1274	1210.901	1241.660
X_2	1700	1711.542	1683.383
Y_2	–260	–296.513	–368.349
X_3	140	260.000	35.061
L_{42}	899	999.526	960.785
L_{45}	1510	1319.051	1598.283
Ang_4	–140	–133.073	–137.104
L_5	2025	1651.916	1558.529

equipped with linkages Lk_4 or Lk_5 is equal to that of SL4-2000A, but the motor and drive system energy consumption is more than 11% lower. Compared with SL4-2000A in constant-eccentric-speed mode (S_{wk} = 300 mm and Nc = 15 s/min), the energy consumption of linkage Lk_5 was reduced by 34.3% and the work rating was increased by 1.12 times per minute. A comparison of motion-planning results between linkage Lk_5 (in constant-slide-speed mode) and SL4-2000A (in constant-eccentric-speed mode) is shown in Fig. 12.

Figure 13 shows that the constant slide speed in *SegWork* of optimized linkage Lk_5 was 250 mm/s and the upper limit of the stroke to maintain this speed was about 260 mm. However, Table 11 shows that linkage Lk_5 can be used for a drawing stroke of 300 mm and the energy consumption is lower than that of a SL4-2000A (this product was designed for a drawing stroke of 300 mm) linkage system, implying that use of this optimization method in constant-slide-speed mode can extend the work capability of a small-stroke linkage.

The results of motion planning for both constant-eccentric-speed and constant-slide-speed modes proved that this method of linkage based on phase division is efficient in improving energy saving and work rating. Using this method, the root-mean-square torque can be lowered,

Table 10 Features of linkages optimized in constant-slide-speed mode

Mechanism	Max work stroke	*SegWork* constant velocity	Die area open angle	System inertia	Mechanism inertia	Mechanism inertia (*SegWork*)	*SegWork* friction power	Ideal equivalent force arm	
	S_c/mm	Vs_{WkC}/(mm·s^{-1})	$\Delta\Phi_{feed}$/(°)	Je_{Max}/(kg·m^2)	Je_{LkMax}/(kg·m^2)	Je_{LkMax}/(kg·m^2)	W_{FrcWk}/kJ	m_{IE13}/mm	m_{IE8}/mm
SL4-2000A	300	≈303	175.3	19900.6	4398.7	3522.3	6040.3	130.7	104.5
Lk_4	300	275	165.0	21889.1	4555.3	3313.5	6037.6	123.4	99.0
Lk_5	260	250	161.0	21088.2	4398.9	3029.1	5945.6	119.5	96.2

Table 11 Motion-planning results for linkages optimized in constant-slide-speed mode

Mechanism	S_{wk}=300		S_{wk}=250	
	Nc_{max}/ (s·min^{-1})	Td_{rms}/ (N·m)	Nc_{max}/ (s·min^{-1})	Td_{rms2}/ (N·m)
SL4-2000A	16.118	6075.4	16.482	6204.1
Lk4	16.087	5637.7	16.419	5694.0
Lk5	16.120	5395.1	16.457	5390.5

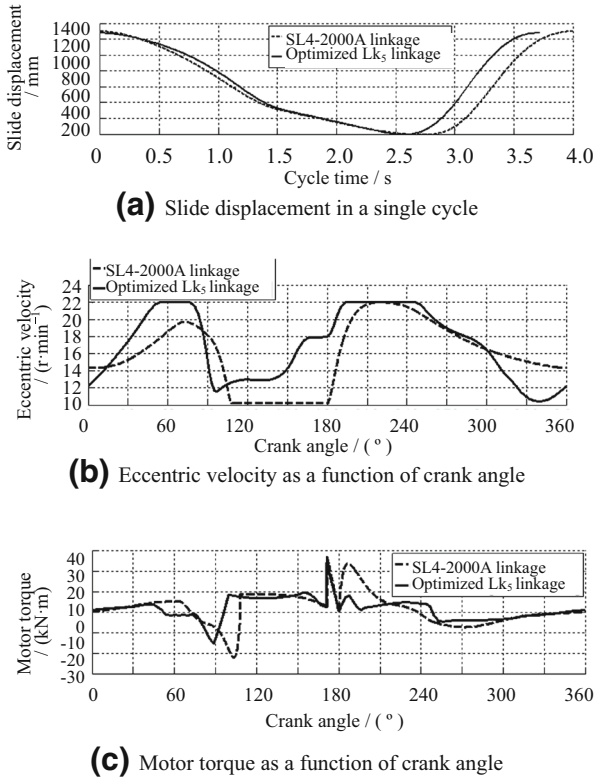

Figure 12 Comparison of motion planning between linkage Lk_5 and SL4-2000A (constant-eccentric-speed mode)

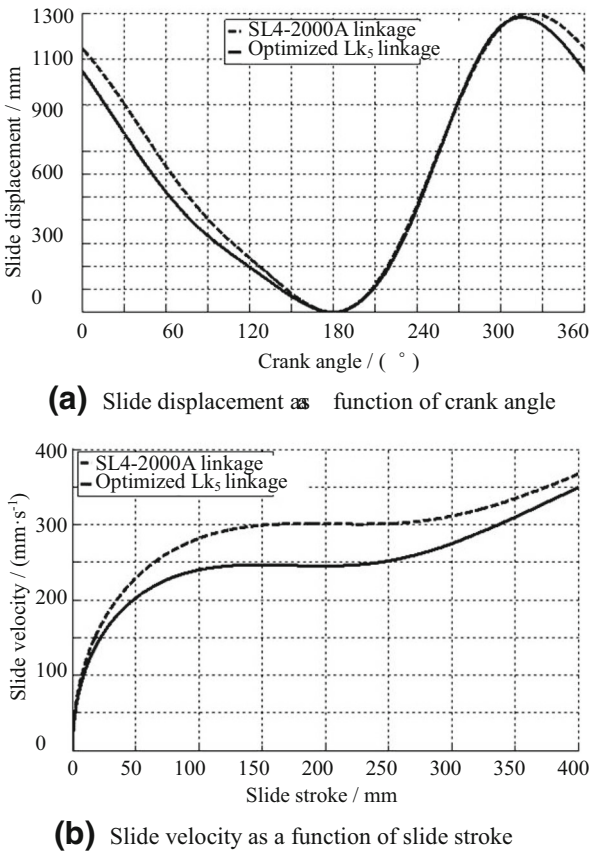

Figure 13 Motion curves for optimized linkage Lk_5 and L4-2000A

which can enable large decreases in drawing servo press manufacturing costs. Although use of constant-slide-speed mode in the *SegWork* phase is an advanced motion-planning technique, it is not yet widely used in practice: this paper could be helpful to its applications in drawing servo presses.

5 Conclusions

1. A new linkage-optimization method for drawing servo presses is proposed, based on phase-division. The objective functions and constraints of the method are established. Starting from any initial value, this method can obtain solutions with high accuracy.
2. Optimization based on constant-eccentric-speed mode was investigated. Linkages were optimized under both the same and different design parameters to those of the SL4-2000A. Comparative results showed that optimization in constant-eccentric-speed mode can lower the root-mean-square torque of the motor, which has implications for significantly reducing the manufacturing costs of drawing servo presses.
3. Optimization in constant-slide-speed mode was systematically investigated. The results showed that optimization in this mode has obvious advantages over constant-eccentric-speed mode in respect of work rating and energy saving.

References

1. D Y He. *Crank press*. Beijing: China Machine Press, 1987. (in Chinese).
2. K Osakada, K Mori, T Altan, et al. Mechanical servo press technology for metal forming. *CIRP Annals-Manufacturing Technology*, 2011, 60: 651–672.
3. Y Xu. Kinematics simulation and optimized design of seven-1ink mechanism of double crank press based on ADAMS. *Journal of Chongqing Technology and Business (Natural Sciences Edition),* 2010, 27(5): 509–512. (in Chinese).
4. H Li, C Zhang, Y M Song. Dynamic formulation and simulation of the programmable press. *Journal of Mechanical Engineering*, 2005, 41(3): 180–184. (in Chinese).
5. J X Qu, Q X Xia, X B Long, et al. Research development on the main drive system and control technologies of servo press. *Forging and Stamping Technology*, 2014, 39(10): 89–97. (in Chinese).
6. Y Fang, Y S Sun, J G Hu, et al. Research on kinematics/dynamics simulation of servo-press transmission mechanism based on MATLAB. *China Mechanical Engineering*, 2012, 23(3): 339–342. (in Chinese).
7. J He, F Gao, Y J Bai, et al. Dynamic modeling and experiment of a new type of parallel servo press considering gravity counterbalance. *Chinese Journal of Mechanical Engineering*, 2013, 26(6): 1222–1233.
8. J Xie, S D Zhao, Z H Sha, et al. Position servo control of the slider in double toggle mechanical press using Bezier curve model and fuzzy control. *IEEE International Conference on Automation Science and Engineering*, Trieste, 2011: 773–778.
9. K Osakada. Application of servo presses to metal forming processes. *Steel Research International*, 2010, 81(9): 9–16.
10. Y J Bai, F Gao, W Z Guo. Design of mechanical presses driven by multi-servomotor. *Journal of Mechanical Science & Technology*, 2011, 25(9): 2323–2334.
11. W Z Guo, F Gao. Design of a servo mechanical press with redundant actuation. *Chinese Journal of Mechanical Engineering*, 2009, 22(4): 574–579.
12. F Meoni, M Carricato. Design of non-overconstraine energy-efficient multi-axis servo presses for deep-drawing applications. *Journal of Mechanical Design*, 2016, 138(6): 065001-1–9.
13. T H Chu, K H Fuh, W C Yeh. Modelling and analysis of deep drawing with utilisation of vibrations and servo press using response surface methodology. *Material Research Innovations*, 2015, 18(S2): S2-936–S2-939.
14. Q Y Song, B F Guo, J Li. Drawing motion profile planning and optimizing for heavy servo press. *The International Journal of Advanced Manufacturing Technology*, 2013, 69(9): 2819–2831.
15. Y H Zhou, F G Xie, X J Liu. Type synthesis and optimization of main driving mechanism for servo-punch press. *Journal of Mechanical Engineering*, 2015, 51(11): 1–7. (in Chinese).
16. Y H Zhou, F G Xie, X J Liu. Optimal design of a main driving mechanism for servo punch press based on performance atlases. *Chinese Journal of Mechanical Engineering*, 2013, 26(5): 909–917.
17. D Mundo, G A Danieli, H S Yan. Kinematic optimization of mechanical presses by optimal synthesis of cam-integrated linkages. *Transactions of the Canadian Society for Mechanical Engineering*, 2006, 30(4): 519–532.
18. R X Du, W Z Guo. The design of a new metal forming press with controllable mechanism. *Journal of Mechanical Design*, 2003, 125(3): 582–592.
19. P L Tso, K C Liang. A nine-bar linkage for mechanical forming presses. International *Journal of Machine Tools & Manufacture*, 2002, 42(1): 139–145.
20. P Groche, M Scheitza, M Kraft, et al. Increased total flexibility by 3D servo presses. *CIRP Annals - Manufacturing Technology*, 2010, 59(1): 267–270.
21. R Matsumoto, S Sawa, H Utsunomiya, et al. Prevention of galling in forming of deep hole with retreat and advance pulse ram motion on servo press. *CIRP Annals - Manufacturing Technology*, 2011, 60(1): 315–318.
22. W Q Chen, D H Huo, W K Xie, et al. Integrated simulation method for interaction between manufacturing process and machine tool. *Chinese Journal of Mechanical Engineering*, 2016, 29(6): 1090–1095.
23. S D Shen. *Practical theory of mechanisms*. Beijing: China Textile Industry Press, 1997. (in Chinese).
24. R L Norton. *Design of machinery an introduction to the synthesis and analysis of mechanisms and machines*. Beijing: China Machine Press, 2003. (in Chinese).
25. Y N Ji, R H Zhang, H H Miu, et al. A study of the mechanized presser simulation movement and the curve movement of slides based on Adams six linkage. *Agriculture Equipment & Technology*, 2013, 39(6): 15–17.
26. X D Chen. Optimization design of mechanical press machine six-link mechanism based on Adams. *Mechanical Drive*, 2016, 40(6): 97–105. (in Chinese).

Zhi-Gang Zhang, born in 1957, is currently a director at *National Key Laboratory for Advanced Intelligent Large Stamping Machines.*

He received his PhD degree from *Tsinghua University, China*. His research interests include the design of mechanical and servo press.

Li-Ping Wang, born in 1967, is currently a professor at *Department of Mechanical Engineering, Tsinghua University, China*. His research interests include advanced manufacturing equipment and its control. E-mail: lpwang@tsinghua.edu.cn

Yan-Ke Cao, born in 1982, is an engineer at *JIER Machine-Tool Group Co., Ltd*. He received his master degree in 2012, and his research interests include design of mechanical and servo press. E-mail:cao_yanke@jiermt.com